

# Water-Compatible and Recyclable Heterogeneous SABRE Catalyst for NMR Signal Amplification

Sein Min, Juhee Baek, Jisu Kim, Hye Jin Jeong, Jean Chung,\* and Keunhong Jeong\*



Cite This: *JACS Au* 2023, 3, 2912–2917



Read Online

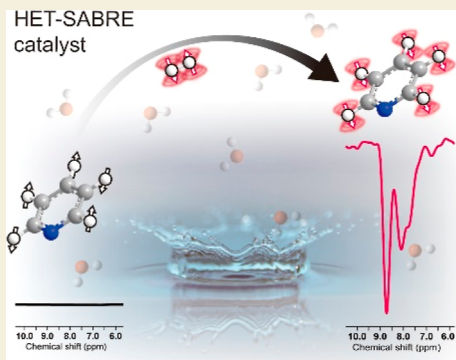
ACCESS |

Metrics & More

Article Recommendations

Supporting Information

**ABSTRACT:** A water-compatible and recyclable catalyst for nuclear magnetic resonance (NMR) hyperpolarization via signal amplification by reversible exchange (SABRE) was developed. The  $[\text{Ir}(\text{COD})(\text{IMes})\text{Cl}]$  catalyst was attached to a polymeric resin of bis(2-pyridyl)amine (heterogeneous SABRE catalyst, HET-SABRE catalyst), and it amplified the  $^1\text{H}$  NMR signal of pyridine up to (–) 4455-fold (43.2%) at 1.4 T in methanol and (–) 50-fold (0.5%) in water. These are the highest amplification factors ever reported among HET-SABRE catalysts and for the first time in aqueous media. Moreover, the HET-SABRE catalyst demonstrated recyclability by retaining its activity in water after more than three uses. This newly designed polymeric resin-based heterogeneous catalyst shows great promise for NMR signal amplification for biomedical NMR and MRI applications in the future.



**KEYWORDS:** NMR, parahydrogen, water hyperpolarization, HET-SABRE, polymeric nanoparticles

## INTRODUCTION

Nuclear magnetic resonance (NMR) and magnetic resonance imaging (MRI) signals may be significantly amplified by inducing highly nonequilibrium nuclear spin polarization (hyperpolarization). Hyperpolarization can overcome the fundamental sensitivity limits of modern NMR/MRI<sup>1–8</sup> and has been used to enhance medical diagnosis, chemical reaction monitoring, development of new materials, and synthesis of pharmaceuticals.<sup>9–14</sup> Among the different hyperpolarization techniques, signal amplification by reversible exchange (SABRE) has been actively developed due to its economical and straightforward setup.<sup>9,15–20</sup> It is capable of obtaining and regenerating hyperpolarization on target materials by using para-state of hydrogen (*para*-hydrogen) in real time.<sup>21</sup> In SABRE, an organometallic catalyst forms a reversible complex between *para*-hydrogen and the target substrate.<sup>22–24</sup> Subsequently, the spin order is spontaneously transferred through the *J*-coupling network without any changes in the substrate's covalent bonds.<sup>25,26</sup> Efficient and regenerative SABRE processes have been mostly carried out using homogeneous catalysts, which is hard to separate for reuse.<sup>9</sup> This is particularly disadvantageous for MRI due to the presence of a toxic organometallic catalyst in the solution after substrate polarization has been achieved.<sup>27,28</sup> Even worse, when a homogeneous SABRE system is activated, prechelated ligands (e.g., octadiene) may be released into the solution. Therefore, developing an efficient SABRE catalyst that is separable from the hyperpolarized product and compatible with aqueous media is crucial for expanded applications in clinical MRI.

Previous studies have investigated separation techniques for homogeneous catalysts and heterogeneous catalysts to improve PHIP used for supported/metal oxide catalysts<sup>29–32</sup> and SABRE's compatibility with medical applications.<sup>33</sup> For example, a homogeneous catalyst was fixed to a solid support through an organic linker. This approach generally involves the linking of the iridium metal to the solid support via weak coordination with pyridine. Goodson and co-workers conducted heterogeneous-SABRE (HET-SABRE) using polymer-bound 4-dimethylaminopyridine and 3-aminopropyl-functionalized silica gel.<sup>33–35</sup> Other advances have been made using similar approaches.<sup>36–40</sup> However, no one to date has demonstrated hyperpolarization efficiency and catalyst reusability generally required for MRI. Most importantly, no solid-supported catalysts have yet demonstrated SABRE activity in water. Thus, developing a water-compatible and recyclable heterogeneous SABRE catalyst with high amplification capability is an important technical challenge.<sup>41,42</sup>

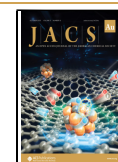
Here, we report a new HET-SABRE catalyst with unprecedented efficiency and regenerative hyperpolarization on pyridine and nicotinamide in methanol and water. The Ir(I) SABRE catalyst was attached to a polymeric resin (TentaGel

**Received:** August 21, 2023

**Revised:** September 20, 2023

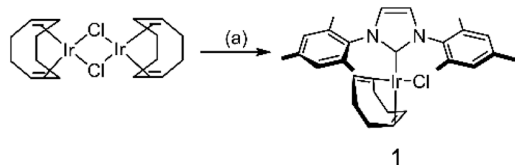
**Accepted:** September 22, 2023

**Published:** October 10, 2023

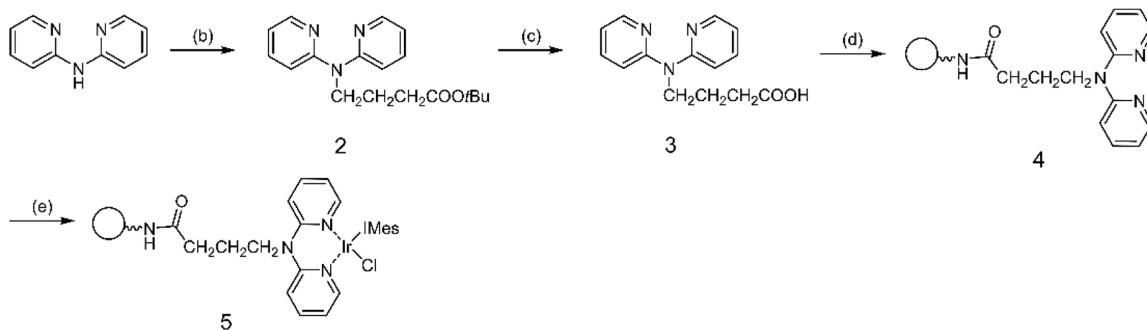


**Scheme 1. Synthesis of SABRE (1), HET-SABRE Pre-catalyst (5).** (a) 1,3-Bis(2,4,6-trimethylphenyl)imidazole-2-ylidene, THF. (b) *t*-Butyl-4-bromobutyrate, KI, KOH, DMF. (c) Trifluoroacetic Acid, DCM. (d) TentaGel S-NH<sub>2</sub>, HCTU, DIEA, DMF. (e) [Ir(COD)(IMes)Cl] (1), MeOH, 24 h

### Homogeneous catalyst



### Heterogeneous catalyst



S), which absorbs both methanol and water. This newly synthesized HET-SABRE catalyst, unlike previous examples, displays an amplification factor similar to that of the homogeneous SABRE catalyst in methanol. In addition, hyperpolarization activity by HET-SABRE catalyst was confirmed in water (D<sub>2</sub>O) for the first time. Although amplification in water is comparatively low, the catalyst shows a regenerative property and opens new possible biological applications.

The HET-SABRE catalyst was synthesized as shown in Scheme 1 (see the figure in Supporting Information for detailed information). First, the homogeneous SABRE catalyst, [Ir(COD)(IMes)Cl] (1), was prepared according to the method reported previously.<sup>41</sup> Then, bis(2-pyridyl)amine (BPA) was functionalized with carboxylic acid via an S<sub>N</sub>2 reaction (2).<sup>43</sup> Then, BPA carboxylic acid (3) and *O*-(1*H*-6-chlorobenzotriazole-1-yl)-1,1,3,3-tetramethyluronium hexafluorophosphate (HCTU) were dissolved in *N,N*-dimethylformamide (DMF). The solution was treated with *N,N*-diisopropylethylamine (DIEA) for activation. TentaGel S-NH<sub>2</sub> resin (Sigma-Aldrich) was mixed with the activated solution for amide coupling for 2 h (d). The resulting resin (4) was monitored with the Kaiser test to confirm the amide coupling, whereby its color turns from purple–blue to bright yellow upon functionalization.<sup>44,45</sup> The solution was filtrated in a plastic column and washed with methanol three times. Then, (1) was dissolved in methanol, and the functionalized resin (4) was combined and shaken for 24 h. It was then filtered and washed again with methanol three times until the supernatant solution was colorless (e). Its color change indicates the successful synthesis of the heterogeneous catalysts (Table S1). The functionalized resin was dried under vacuum to give the HET-SABRE precatalyst, which is dark yellow (Table S1, 5).

In our previous SABRE study,<sup>46</sup> it was difficult to observe strong signal amplification on BPA substrates itself because of their strong binding affinity to the catalyst. Also, we conducted a theoretical study to estimate the plausible structure of the

polarization transfer mechanism. Building upon previous studies that utilized DFT (density functional theory) calculations,<sup>47,48</sup> we investigated the theoretical aspects further. Specifically, we examined two different cases involving the stabilization of the structures of BPA and pyridine with the Ir-catalyst and pyridine with an equatorial structure and found that the pyridine was slightly more stable when it was in the equatorial position (Figure S8). Therefore, we developed a new catalyst with a strong coordinated iridium catalyst, and the spectrum obtained with the resin is shown in Figure 1.

Importantly, the Ir(I) catalyst is strongly bound to the functionalized resin, indicated by the dark yellow color of the resin. In contrast, the solution of methanol and pyridine stays colorless and transparent during SABRE. From the hyperpolarized spectrum, no hydride peaks [around (–) 12 to (–) 30 ppm] were seen, which indicates that SABRE is only done by the solid supported catalyst (Figure S7a,c). Remarkably, the amplification factors were similar to those obtained by homogeneous catalysts, indicating high efficiency. In addition, the catalyst activation time is also similar, at about 300 s (Figure 1c). The external magnetic field greatly affected the efficiency of SABRE (see the figures in the Supporting Information for detailed information, Figures S4 and S5). The HET-SABRE spectrum clearly appeared as the highly intensified signal on the pyridine substrate, and ortho, para, and meta <sup>1</sup>H positions around the pyridine ring were ~ (–) 27.9, (–) 21.2, and (–) 43.2%, respectively. Indeed, optimization at various concentrations and magnetic fields established the greatest polarization (%) at 1.4 mM in 70 G, confirming the possibility of HET-SABRE in methanol.

In addition, inductively coupled plasma mass spectrometry (ICP/MS) analysis was performed to check the recyclability of the HET-SABRE catalyst by measuring the iridium content on the supernatant of the solution for each SABRE (Table S2). For three recycling procedures, the iridium levels were very low compared to the reference solution of the SABRE catalyst in methanol, which indicates that the iridium catalyst is

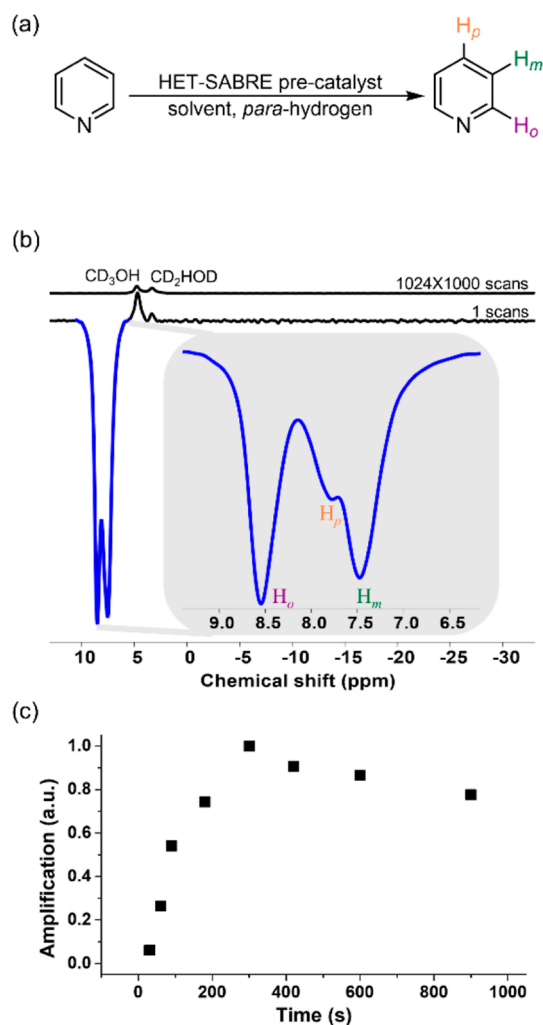


**Figure 1.** (a) Schematic of HET-SABRE showing  $^1\text{H}$  pyridine and *para*-hydrogen exchange on the activated HET-SABRE precatalyst (5) producing efficient  $^1\text{H}$  hyperpolarization. (b) 1.4 mM pyridine was hyperpolarized with 8 mg of catalyst via HET-SABRE in methanol- $d_4$  using 1 atm of *para*-hydrogen.  $^1\text{H}$  NMR spectrum without hyperpolarization (black, 1024 scans and plotted 1000 $\times$ ) and with HET-SABRE (blue) is shown in Figure 1. Amplification factors  $\epsilon$  were (–) 2881, (–) 2189, and (–) 4455-fold, corresponding to (–) 27.9, (–) 21.2, and (–) 43.2%, for  $\text{H}_o$ ,  $\text{H}_p$ , and  $\text{H}_m$ , respectively. (c) Optimized hyperpolarized activation time.

strongly coordinated to the resin during recycling and supports the development of the sustainable HET-SABRE.

Motivated by the biological application of SABRE hyperpolarization techniques, we performed HET-SABRE hyperpolarization in water ( $\text{D}_2\text{O}$ ). It was confirmed that the  $^1\text{H}$  NMR signal of pyridine in  $\text{D}_2\text{O}$  was amplified up to (–) 53-fold at 70 G (Figure 2b and S5). We also note that this is the highest amplification number from the results achieved using even the water-soluble catalyst (homogeneous catalyst) following dissolution and activation.<sup>38–40,42</sup> These results indicate the successful demonstration of a catalyst capable of performing HET-SABRE in aqueous media in one step.

It is noteworthy that SABRE-based hyperpolarization on pyridine in water is possible despite the low solubility of hydrogen gas in water.<sup>40,42</sup> Further, since the Ir(I)-catalyst is insoluble and inactive in water, the hyperpolarization by the

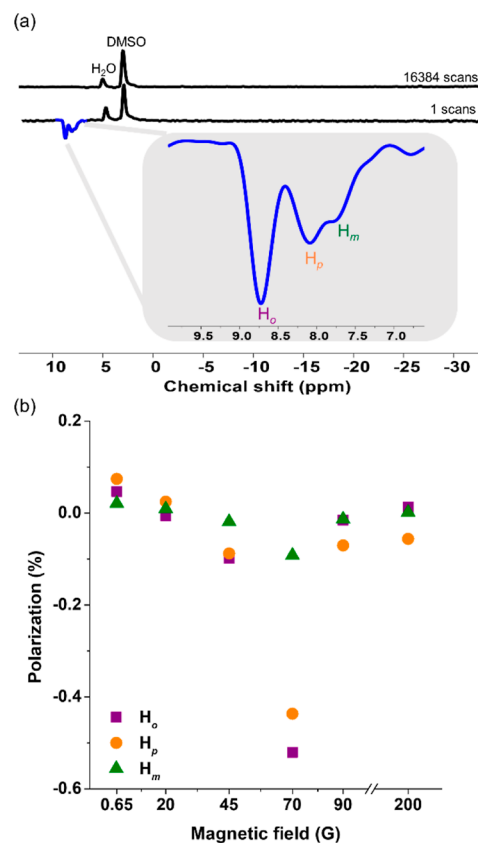


**Figure 2.** (a)  $^1\text{H}$  NMR spectrum of HET-SABRE in water. Hyperpolarized 1.4 mM pyridine (8 mg catalyst) via HET-SABRE in  $\text{D}_2\text{O}$  (with 10  $\mu\text{L}$  of  $\text{DMSO-}d_6$  as the reference) using 1 atm of *para*-hydrogen. [Amplification factor  $\epsilon$  = (–) 53, (–) 45, and (–) 9.5-fold, corresponding to polarization = (–) 0.51, (–) 0.44, and (–) 0.09%, for  $\text{H}_o$ ,  $\text{H}_p$ , and  $\text{H}_m$ , respectively.] The black line is a thermal NMR signal averaged over 16,384 scans, and the blue line is a hyperpolarized NMR signal in 1 scan. (b)  $^1\text{H}$  hyperpolarized 1.4 mM pyridine polarization in various magnetic fields.

HET-SABRE catalyst demonstrates its high efficiency and strong binding to the resin.

In addition to high hyperpolarization efficiency and compatibility with water, the new catalyst design demonstrates successful separation and recyclability of heterogeneous catalysts (Figure 3). During the recycling procedure, the reused HET-SABRE catalysts showed similar efficiencies in each measurement, demonstrating that continuous hyperpolarization in water is possible.

Nicotinamide (vitamin B3 amide), which has low in vivo toxicity, is potentially an attractive molecular imaging target.<sup>49,50</sup> It significantly can be utilized to improve the resolution of future studies with hyperpolarized nicotinamide. It was confirmed that the  $^1\text{H}$  NMR signal of nicotinamide in  $\text{D}_2\text{O}$  was amplified up to (–) 0.44% at 70 G (Figures 4b and S6). These data suggest that various compounds can be hyperpolarized in water through the HET-SABRE precatalyst.

A unique solid-supported organometallic iridium catalyst for SABRE was successfully developed and demonstrated enhancement of the  $^1\text{H}$  NMR signal of pyridine in both methanol and water for the first time, which can be used continuously in a flowing system.  $^1\text{H}$  signal amplification between (–) 2000 and (–) 4000-fold (more than 40%) was obtained from newly synthesized HET-SABRE catalysts in methanol, which

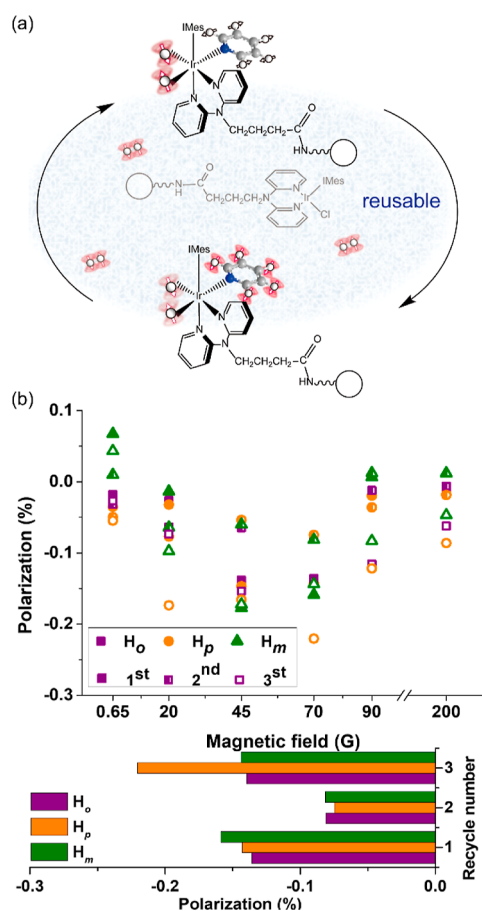


**Figure 3.** (a) Catalyst recycling via HET-SABRE hyperpolarization on pyridine. (b)  $^1\text{H}$  hyperpolarized 14 mM pyridine polarization (%) using  $\text{D}_2\text{O}$ . Indicates the efficiency of the reused catalyst. Polarization of pyridine proton sites at 70 G using the reused catalyst.

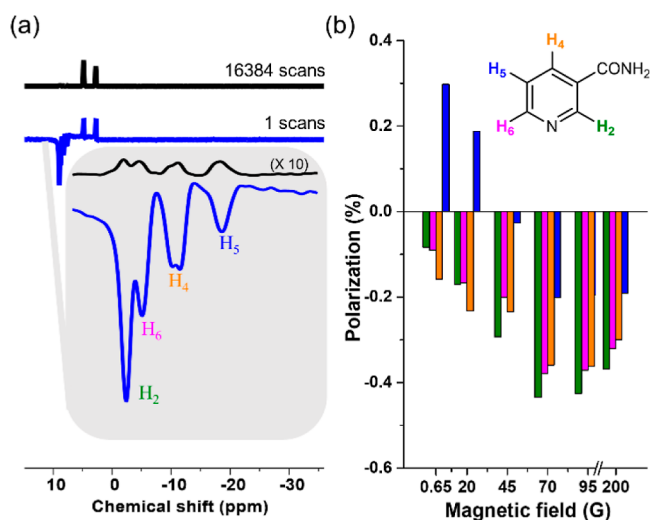


**Figure 4.** (a)  $^1\text{H}$  NMR spectrum of HET-SABRE in water. Hyperpolarized 1.4 mM nicotinamide (8 mg catalyst) via HET-SABRE in  $\text{D}_2\text{O}$  (with 10  $\mu\text{L}$  of  $\text{DMSO}-d_6$  as the reference) at 70 G using 100% *para*-hydrogen. [(−) 0.43, (−) 0.37, (−) 0.36, and (−) 0.20% for  $H_2$ ,  $H_4$ ,  $H_5$ , and  $H_6$ , respectively.] The black line is a thermal NMR signal averaged over 16,384 scans ( $\times 10$ ), and the blue line is a hyperpolarized NMR signal in 1 scan. (b)  $^1\text{H}$  hyperpolarized 1.4 mM nicotinamide polarization in various magnetic fields.

dramatically advanced the current HET-SABRE approach. In fact, by optimizing the *para*-hydrogen gas pressure and various experimental conditions (e.g., polymer support particle size, total catalyst concentration on solid-support, etc.), larger NMR signal enhancement may be expected in the future. Unlike conventional catalysts, they enable easy separation and recycling of the SABRE catalyst in solution, and the removal of unwanted chelating ligands has already been addressed in advance.

The newly developed HET-SABRE catalyst here was also used to induce the real-time hyperpolarization of pyridine and nicotinamide in aqueous media. This will ultimately enable hyperpolarized biomolecules in biomedical water.<sup>51,52</sup> Indeed, our efforts not only improve signal enhancement through these experimental optimizations but also identify SABRE-based real-time hyperpolarization of biological/biomedical materials in a heterogeneous system.

## METHODS

### Sample Preparation

Most of the reagents used in this work were purchased from Sigma-Aldrich, Alfa Aesar, Tokyo Chemical Industry, and other companies. The samples used for the SABRE experiments contained 8 mg of the HET-SABRE precatalyst (**5**) and the selected substrate, either pyridine or nicotinamide (Sigma-Aldrich). The catalysts were chosen following optimization. The solvents were methanol- $d_4$  (Euriscotop) and water- $d_2$  (Euriscotop). The total sample volume was 0.9 mL.

### HET-SABRE Experiments

All the experiments presented in this article were carried out using a Nanalysis 60 MHz spectrometer or a Bruker 300 MHz spectrometer and referenced to the residual solvent peak of methanol- $d_4$  ( $\delta = 3.31$  ppm) and water- $d_2$  ( $\delta = 4.79$  ppm) with a permanent magnet at room temperature. The mostly used *para*-hydrogen generator was enriched to  $\sim 50\%$  similarly as described previously and stored in Dewar containers to be used on demand ( $\sim 100\%$  *para*-hydrogen was used for nicotinic amide).

8 mg of the HET-SABRE precatalyst (**5**) was placed in a 5 mm NMR tube fitted with a J. Young's cap along with various pyridine concentrations dissolved in 900  $\mu\text{L}$  of the NMR solvent. After *para*-hydrogen bubbling within the various magnetic fields, the sample was quickly transferred to the NMR spectrometer, and an enhanced signal was detected. Results were obtained by a 90-degree proton pulse using "zg 90" using one scan. The NMR data were analyzed by Mnova Software (Mestrelab Research, S.L.).

## ASSOCIATED CONTENT

### Supporting Information

The Supporting Information is available free of charge at <https://pubs.acs.org/doi/10.1021/jacsau.3c00487>.

Synthesis and characterization of the HET-SABRE catalyst, SABRE experimental setup, hyperpolarization data analysis, and DFT calculations (PDF)

## AUTHOR INFORMATION

### Corresponding Authors

**Keunhong Jeong** – Department of Chemistry, Korea Military Academy, Seoul 01805, South Korea; [orcid.org/0000-0003-1485-7235](https://orcid.org/0000-0003-1485-7235); Email: [jkchung@colostate.edu](mailto:jkchung@colostate.edu)

**Jean Chung** – Department of Chemistry, Colorado State University, Fort Collins, Colorado 80523, United States; [orcid.org/0000-0001-8221-0500](https://orcid.org/0000-0001-8221-0500); Email: [doas1mind@kma.ac.kr](mailto:doas1mind@kma.ac.kr)

## Authors

**Sein Min** – Department of Chemistry, Seoul Women's University, Seoul 01797, South Korea

**Juhée Baek** – Department of Chemistry, Seoul Women's University, Seoul 01797, South Korea

**Jisu Kim** – Department of Chemistry, Seoul Women's University, Seoul 01797, South Korea

**Hye Jin Jeong** – Department of Chemistry, Colorado State University, Fort Collins, Colorado 80523, United States

Complete contact information is available at:

<https://pubs.acs.org/10.1021/jacsau.3c00487>

## Author Contributions

CRedit: **Sein Min** data curation, formal analysis, investigation, writing-original draft; **Juhée Baek** data curation, investigation, methodology; **Jisu Kim** data curation, investigation, methodology; **Hye Jin Jeong** data curation, investigation, methodology; **Jean Chung** conceptualization, investigation, project administration, supervision, writing-original draft, writing-review & editing; **Keunhong Jeong** conceptualization, funding acquisition, investigation, project administration, resources, supervision, writing-original draft, writing-review & editing.

## Notes

The authors declare no competing financial interest.

## ACKNOWLEDGMENTS

This research was supported by the National Research Foundation of Korea (NRF) grant funded by the Korean government (MSIT) (no. 2020R1C1C1007888).

## REFERENCES

- (1) Song, C.; Hu, K. N.; Joo, C. G.; Swager, T. M.; Griffin, R. G. TOTAPOL: A Biradical Polarizing Agent for Dynamic Nuclear Polarization Experiments in Aqueous Media. *J. Am. Chem. Soc.* **2006**, *128* (35), 11385–11390.
- (2) Maly, T.; Debelouchina, G. T.; Bajaj, V. S.; Hu, K. N.; Joo, C. G.; Mak-Jurkauskas, M. L.; Sirigiri, J. R.; Van Der Wel, P. C. A.; Herzfeld, J.; Temkin, R. J.; Griffin, R. G. Dynamic Nuclear Polarization at High Magnetic Fields. *J. Chem. Phys.* **2008**, *128* (5), 052211.
- (3) Walker, T. G.; Happer, W. Spin-Exchange Optical Pumping of Noble-Gas Nuclei. *Rev. Mod. Phys.* **1997**, *69* (2), 629–642.
- (4) Goodson, B. M. Nuclear Magnetic Resonance of Laser-Polarized Noble Gases in Molecules, Materials, and Organisms. *J. Magn. Reson.* **2002**, *155* (2), 157–216.
- (5) Koptyug, I. V.; Kovtunov, K. V.; Burt, S. R.; Anwar, M. S.; Hilty, C.; Han, S. I.; Pines, A.; Sagdeev, R. Z. Para-Hydrogen-Induced Polarization in Heterogeneous Hydrogenation Reactions. *J. Am. Chem. Soc.* **2007**, *129* (17), 5580–5586.
- (6) Duckett, S. B.; Mewis, R. E. Application of Para Hydrogen Induced Polarization Techniques in NMR Spectroscopy and Imaging. *Acc. Chem. Res.* **2012**, *45* (8), 1247–1257.
- (7) Eisenberg, R. Parahydrogen-Induced Polarization: A New Spin on Reactions with H<sub>2</sub>. *Acc. Chem. Res.* **1991**, *24* (4), 110–116.
- (8) Duckett, S. B.; Blazina, D. The Study of Inorganic Systems by NMR Spectroscopy in Conjunction with Parahydrogen-Induced Polarization. *Eur. J. Inorg. Chem.* **2003**, *2003* (16), 2901–2912.
- (9) Adams, R. W.; Aguilar, J. A.; Atkinson, K. D.; Cowley, M. J.; Elliott, P. I. P.; Duckett, S. B.; Green, G. G. R.; Khazal, I. G.; López-Serrano, J.; Williamson, D. C. Reversible Interactions with Para-Hydrogen Enhance NMR Sensitivity by Polarization Transfer. *Science* **2009**, *323* (5922), 1708–1711.
- (10) Lee, J. H.; Okuno, Y.; Cavagnero, S. Sensitivity Enhancement in Solution NMR: Emerging Ideas and New Frontiers. *J. Magn. Reson.* **2014**, *241* (1), 18–31.
- (11) Christensen, C. E.; Karlsson, M.; Winther, J. R.; Jensen, P. R.; Lerche, M. H. Non-Invasive in-Cell Determination of Free Cytosolic [NAD<sup>+</sup>]/[NADH] Ratios Using Hyperpolarized Glucose Show Large Variations in Metabolic Phenotypes. *J. Biol. Chem.* **2014**, *289* (4), 2344–2352.
- (12) Stern, Q.; Milani, J.; Vuichoud, B.; Bornet, A.; Gossert, A. D.; Bodenhausen, G.; Jannin, S. Hyperpolarized Water to Study Protein-Ligand Interactions. *J. Phys. Chem. Lett.* **2015**, *6* (9), 1674–1678.
- (13) Harris, T.; Szekeley, O.; Frydman, L. On the Potential of Hyperpolarized Water in Biomolecular NMR Studies. *J. Phys. Chem. B* **2014**, *118* (12), 3281–3290.
- (14) Kurhanewicz, J.; Vigneron, D. B.; Brindle, K.; Chekmenev, E. Y.; Comment, A.; Cunningham, C. H.; DeBerardinis, R. J.; Green, G. G.; Leach, M. O.; Rajan, S. S.; Rizi, R. R.; Ross, B. D.; Warren, W. S.; Malloy, C. R. Analysis of Cancer Metabolism by Imaging Hyperpolarized Nuclei: Prospects for Translation to Clinical Research. *Neoplasia* **2011**, *13* (2), 81–97.
- (15) Eshuis, N.; Hermkens, N.; van Weerdenburg, B. J. A.; Feiters, M. C.; Rutjes, F. P. J. T.; Wijmenga, S. S.; Tessari, M. Toward Nanomolar Detection by NMR Through SABRE Hyperpolarization. *J. Am. Chem. Soc.* **2014**, *136* (7), 2695–2698.
- (16) Ratajczyk, T.; Gutmann, T.; Bernatowicz, P.; Buntkowsky, G.; Frydel, J.; Fedorczyk, B. NMR Signal Enhancement by Effective SABRE Labeling of Oligopeptides. *Chem.—Eur. J.* **2015**, *21* (36), 12616–12619.
- (17) Rovedo, P.; Knecht, S.; Bäumlisberger, T.; Cremer, A. L.; Duckett, S. B.; Mewis, R. E.; Green, G. G. R.; Burns, M.; Rayner, P. J.; Leibfritz, D.; Korvink, J. G.; Hennig, J.; Pütz, G.; Von Elverfeldt, D.; Hövener, J. B. Molecular MRI in the Earth's Magnetic Field Using Continuous Hyperpolarization of a Biomolecule in Water. *J. Phys. Chem. B* **2016**, *120* (25), 5670–5677.
- (18) Lee, S. J.; Jeong, K.; Shim, J. H.; Lee, H. J.; Min, S.; Chae, H.; Namgoong, S. K.; Kim, K. SQUID-Based Ultralow-Field MRI of a Hyperpolarized Material Using Signal Amplification by Reversible Exchange. *Sci. Rep.* **2019**, *9*, 12422.
- (19) Hövener, J.; Pravdivtsev, A. N.; Kidd, B.; Bowers, C. R.; Glöggl, S.; Kovtunov, K. V.; Plaumann, M.; Katz-Brull, R.; Buckenmaier, K.; Jerschow, A.; Reineri, F.; Theis, T.; Shchepin, R. V.; Wagner, S.; Bhattacharya, P.; Zacharias, N. M.; Chekmenev, E. Y. Parahydrogen-Based Hyperpolarization for Biomedicine. *Angew. Chem., Int. Ed.* **2018**, *57*, 11140–11162.
- (20) Theis, T.; Ortiz, G. X.; Logan, A. W. J.; Claytor, K. E.; Feng, Y.; Huhn, W. P.; Blum, V.; Malcolmson, S. J.; Chekmenev, E. Y.; Wang, Q.; Warren, W. S. Direct and Cost-Efficient Hyperpolarization of Long-Lived Nuclear Spin States on Universal 15N2-Diazirine Molecular Tags. *Sci. Adv.* **2016**, *2* (3), No. e1501438.
- (21) Knecht, S.; Kiryutin, A. S.; Yurkovskaya, A. V.; Ivanov, K. L. Mechanism of Spontaneous Polarization Transfer in High-Field SABRE Experiments. *J. Magn. Reson.* **2018**, *287*, 74–81.
- (22) Adams, R. W.; Duckett, S. B.; Green, R. A.; Williamson, D. C.; Green, G. G. R. A Theoretical Basis for Spontaneous Polarization Transfer in Non-Hydrogenative Parahydrogen-Induced Polarization. *J. Chem. Phys.* **2009**, *131* (19), 194505.
- (23) Eshuis, N.; Aspers, R. L. E. G.; Van Weerdenburg, B. J. A.; Feiters, M. C.; Rutjes, F. P. J. T.; Wijmenga, S. S.; Tessari, M. Determination of Long-Range Scalar 1H-1H Coupling Constants Responsible for Polarization Transfer in SABRE. *J. Magn. Reson.* **2016**, *265*, 59–66.
- (24) Barskiy, D. A.; Pravdivtsev, A. N.; Ivanov, K. L.; Kovtunov, K. V.; Koptyug, I. V. A Simple Analytical Model for Signal Amplification by Reversible Exchange (SABRE) Process. *Phys. Chem. Chem. Phys.* **2016**, *18* (1), 89–93.
- (25) Lloyd, L. S.; Asghar, A.; Burns, M. J.; Charlton, A.; Coombes, S.; Cowley, M. J.; Dear, G. J.; Duckett, S. B.; Genov, G. R.; Green, G. G. R.; Highton, L. A. R.; Hooper, A. J. J.; Khan, M.; Khazal, I. G.; Lewis, R. J.; Mewis, R. E.; Roberts, A. D.; Ruddlesden, A. J. Hyperpolarisation through Reversible Interactions with Parahydrogen. *Catal. Sci. Technol.* **2014**, *4* (10), 3544–3554.

- (26) Lindale, J. R.; Eriksson, S. L.; Tanner, C. P. N.; Zhou, Z.; Colell, J. F. P.; Zhang, G.; Bae, J.; Chekmenev, E. Y.; Theis, T.; Warren, W. S. Unveiling Coherently Driven Hyperpolarization Dynamics in Signal Amplification by Reversible Exchange. *Nat. Commun.* **2019**, *10* (1), 395–397.
- (27) Manoharan, A.; Rayner, P. J.; Fekete, M.; Iali, W.; Norcott, P.; Hugh Perry, V.; Duckett, S. B. Catalyst-Substrate Effects on Biocompatible SABRE Hyperpolarization. *ChemPhysChem* **2019**, *20* (2), 285–294.
- (28) Manoharan, A.; Rayner, P. J.; Iali, W.; Burns, M. J.; Perry, V. H.; Duckett, S. B. Achieving Biocompatible SABRE: An in Vitro Cytotoxicity Study. *ChemMedChem* **2018**, *13* (4), 352–359.
- (29) Kovtunov, K. V.; Zhivonitko, V. V.; Corma, A.; Koptuyg, I. V. Parahydrogen-Induced Polarization in Heterogeneous Hydrogenations Catalyzed by an Immobilized Au(III) Complex. *J. Phys. Chem. Lett.* **2010**, *1* (11), 1705–1708.
- (30) Kovtunov, K. V.; Beck, I. E.; Bukhtiyarov, V. I.; Koptuyg, I. V. Observation of Parahydrogen-Induced Polarization in Heterogeneous Hydrogenation on Supported Metal Catalysts. *Angew. Chem., Int. Ed.* **2008**, *47* (8), 1492–1495.
- (31) Koptuyg, I. V.; Kovtunov, K. V.; Burt, S. R.; Anwar, M. S.; Hilty, C.; Han, S. I.; Pines, A.; Sagdeev, R. Z. Para-Hydrogen-Induced Polarization in Heterogeneous Hydrogenation Reactions. *J. Am. Chem. Soc.* **2007**, *129* (17), 5580–5586.
- (32) Bales, L. B.; Kovtunov, K. V.; Barskiy, D. A.; Shchepin, R. V.; Coffey, A. M.; Kovtunova, L. M.; Bukhtiyarov, A. V.; Feldman, M. A.; Bukhtiyarov, V. I.; Chekmenev, E. Y.; Koptuyg, I. V.; Goodson, B. M. Aqueous, Heterogeneous para-Hydrogen-Induced 15N Polarization. *J. Phys. Chem. C* **2017**, *121* (28), 15304–15309.
- (33) Shi, F.; Coffey, A. M.; Waddell, K. W.; Chekmenev, E. Y.; Goodson, B. M. Heterogeneous Solution NMR Signal Amplification by Reversible Exchange. *Angew. Chem., Int. Ed.* **2014**, *53* (29), 7495–7498.
- (34) Kovtunov, K. V.; Kovtunova, L. M.; Gemeinhardt, M. E.; Bukhtiyarov, A. V.; Gesiorski, J.; Bukhtiyarov, V. I.; Chekmenev, E. Y.; Koptuyg, I. V.; Goodson, B. M. Heterogeneous Microtesla SABRE Enhancement of 15 N NMR Signals. *Angew. Chem., Int. Ed.* **2017**, *56* (35), 10433–10437.
- (35) Shi, F.; Coffey, A. M.; Waddell, K. W.; Chekmenev, E. Y.; Goodson, B. M. Nanoscale Catalysts for NMR Signal Enhancement by Reversible Exchange. *J. Phys. Chem. C* **2015**, *119* (13), 7525–7533.
- (36) Kidd, B. E.; Gesiorski, J. L.; Gemeinhardt, M. E.; Shchepin, R. V.; Kovtunov, K. V.; Koptuyg, I. V.; Chekmenev, E. Y.; Goodson, B. M. Facile Removal of Homogeneous SABRE Catalysts for Purifying Hyperpolarized Metronidazole, a Potential Hypoxia Sensor. *J. Phys. Chem. C* **2018**, *122* (29), 16848–16852.
- (37) Iali, W.; Oлару, A. M.; Green, G. G. R.; Duckett, S. B. Achieving High Levels of NMR-Hyperpolarization in Aqueous Media With Minimal Catalyst Contamination Using SABRE. *Chem.—Eur. J.* **2017**, *23* (44), 10491–10495.
- (38) Shi, F.; He, P.; Best, Q. A.; Groome, K.; Truong, M. L.; Coffey, A. M.; Zimay, G.; Shchepin, R. V.; Waddell, K. W.; Chekmenev, E. Y.; Goodson, B. M. Aqueous NMR Signal Enhancement by Reversible Exchange in a Single Step Using Water-Soluble Catalysts. *J. Phys. Chem. C* **2016**, *120* (22), 12149–12156.
- (39) Spanning, P.; Reile, I.; Emondts, M.; Schleker, P. P. M.; Hermkens, N. K. J.; van der Zwaluw, N. G. J.; van Weerdenburg, B. J. A.; Tinnemans, P.; Tessari, M.; Blümich, B.; Rutjes, F. P. J. T.; Feiters, M. C. A New Ir-NHC Catalyst for Signal Amplification by Reversible Exchange in D<sub>2</sub>O. *Chem.—Eur. J.* **2016**, *22* (27), 9277–9282.
- (40) Fekete, M.; Gibard, C.; Dear, G. J.; Green, G. G. R.; Hooper, A. J. J.; Roberts, A. D.; Cisnetti, F.; Duckett, S. B. Utilisation of Water Soluble Iridium Catalysts for Signal Amplification by Reversible Exchange. *Dalton Trans.* **2015**, *44* (17), 7870–7880.
- (41) Schmidt, A. B.; de Maissin, H.; Adelabu, I.; Nantogma, S.; Etedgui, J.; TomHon, P.; Goodson, B. M.; Theis, T.; Chekmenev, E. Y. Catalyst-Free Aqueous Hyperpolarized [1-<sup>13</sup>C]Pyruvate Obtained by Re-Dissolution Signal Amplification by Reversible Exchange [<sup>13</sup>C]-Pyruvate Obtained by Re-Dissolution Signal Amplification by Reversible Exchange. *ACS Sens.* **2022**, *7* (11), 3430–3439.
- (42) Truong, M. L.; Shi, F.; He, P.; Yuan, B.; Plunkett, K. N.; Coffey, A. M.; Shchepin, R. V.; Barskiy, D. A.; Kovtunov, K. V.; Koptuyg, I. V.; Waddell, K. W.; Goodson, B. M.; Chekmenev, E. Y. Irreversible Catalyst Activation Enables Hyperpolarization and Water Solubility for NMR Signal Amplification by Reversible Exchange. *J. Phys. Chem. B* **2014**, *118*, 13882–13889.
- (43) Rayner, P. J.; Norcott, P.; Appleby, K. M.; Iali, W.; John, R. O.; Hart, S. J.; Whitwood, A. C.; Duckett, S. B. Fine-Tuning the Efficiency of Para-Hydrogen-Induced Hyperpolarization by Rational N-Heterocyclic Carbene Design. *Nat. Commun.* **2018**, *9* (1), 4251–4311.
- (44) Kirin, S. I.; Yennawar, H. P.; Williams, M. E. Synthesis and Characterization of CuII Complexes with Amino Acid Substituted Di(2-Pyridyl)Amine Ligands. *Eur. J. Inorg. Chem.* **2007**, *2007* (23), 3686–3694.
- (45) Kaiser, E.; Colescott, R.; Bossinger, C.; Cook, P. Color Test for Detection of Free Terminal Amino Groups in the Solid-Phase Synthesis of Peptides. *Anal. Biochem.* **1970**, *34*, 595–598.
- (46) Sarin, V. K.; Kent, S. B. H.; Tam, J. P.; Merrifield, R. B. Quantitative Monitoring of Solid-Phase Peptide Synthesis by the Ninhydrin Reaction. *Anal. Biochem.* **1981**, *117* (1), 147–157.
- (47) Min, S.; Chae, H.; Jeong, H. J.; Kim, K.; Namgoong, S. K.; Jeong, K. Optimization of Signal Amplification by Reversible Exchange for Polarization of Tridentate Chelating Bis[(2-Pyridyl)-Alkyl]Amine. *Analyst* **2021**, *146* (7), 2368–2373.
- (48) Jeong, H. J.; Min, S.; Chae, H.; Kim, S.; Lee, G.; Namgoong, S. K.; Jeong, K. Signal amplification by reversible exchange for COVID-19 antiviral drug candidates. *Sci. Rep.* **2020**, *10* (1), 14290.
- (49) Libri, V.; Yandim, C.; Athanasopoulos, S.; Loyse, N.; Natisvili, T.; Law, P. P.; Chan, P. K.; Mohammad, T.; Mauri, M.; Tam, K. T.; et al. Epigenetic and neurological effects and safety of high-dose nicotinamide in patients with Friedreich's ataxia: an exploratory, open-label, dose-escalation study. *Lancet* **2014**, *384*, 504–513.
- (50) Guyton, J. R.; Blazing, M. A.; Hagar, J. Extended-release niacin vs gemfibrozil for the treatment of low levels of high-density lipoprotein cholesterol. *Arch. Int. Med.* **2000**, *160*, 1177–1184.
- (51) de Maissin, H.; Groß, P. R.; Mohiuddin, O.; Weigt, M.; Nagel, L.; Herzog, M.; Wang, Z.; Willing, R.; Reichardt, W.; Pichotka, M.; Heß, L.; Reinheckel, T.; Jessen, H. J.; Zeiser, R.; Bock, M.; von Elverfeldt, D.; Zaitsev, M.; Korchak, S.; Glöggler, S.; Hövener, J.-B.; Chekmenev, E. Y.; Schilling, F.; Knecht, S.; Schmidt, A. B. In Vivo Metabolic Imaging of [1-<sup>13</sup>C]Pyruvate-d<sub>3</sub> Hyperpolarized by Reversible Exchange With Parahydrogen. *Angew. Chem., Int. Ed.* **2023**, *62*, No. e202306654.
- (52) MacCulloch, K.; Browning, A.; Guarin Bedoya, D.; McBride, S. J.; Abdulmojeed, M. B.; Dedesma, C.; Goodson, B. M.; Rosen, M. S.; Chekmenev, E. Y.; Yen, Y. F.; et al. Facile hyperpolarization chemistry for molecular imaging and metabolic tracking of [1-<sup>13</sup>C]pyruvate in vivo. *ChemRxiv* **2023**, *16–17*, 100129.